



# Fermi National Accelerator Laboratory

FERMILAB-Conf-88/160-E

[E-744]

## Neutrino Production of Charm at FNAL E744\*

C. Foudas, K. T. Bachmann, R. H. Bernstein, R. E. Blair,  
W. C. Lefmann, W. C. Leung, S. R. Mishra, E. Oltman,  
P. Z. Quintas, F. Sciulli, M. H. Shaevitz, W. H. Smith  
Columbia University  
New York, NY 10027

F. S. Merritt, M. Oreglia, H. Schellman, B. A. Schumm  
Enrico Fermi Institute, The University of Chicago  
Chicago, IL 60637

F. Borcharding, H. E. Fisk, M. J. Lamm,  
W. Marsh, K. W. B. Merritt, D. Yovanovich  
Fermi National Accelerator Laboratory  
P.O. Box 500, Batavia, Illinois 60510

A. Bodek, H. S. Budd, W. K. Sakumoto  
University of Rochester  
Rochester, NY 14627

October 1988

\*Talk presented by Heidi Schellman at the SLAC Summer Institute on Particle Physics, July 28, 1988.



**NEUTRINO PRODUCTION of CHARM at FNAL E744**

C. Foudas, K. T. Bachmann, R. H. Bernstein, R. E. Blair,  
W. C. Lefmann, W. C. Leung, S. R. Mishra, E. Oltman,  
P. Z. Quintas, F. Sciulli, M. H. Shaevitz, W. H. Smith  
**Columbia University**

F. S. Merritt, M. Oreglia, H. Schellman, B. A. Schumm  
**Enrico Fermi Institute, University of Chicago**

F. Borcharding, H. E. Fisk, M. J. Lamm,  
W. Marsh, K. W. B. Merritt, D. Yovanovitch  
**Fermi National Accelerator Laboratory**

A. Bodek, H. S. Budd, W. K. Sakumoto  
**University of Rochester**

*Talk presented by Heidi Schellman at the SLAC Summer Institute on Particle Physics , July 28, 1988.*

**ABSTRACT**

We present data on opposite-sign dimuon production in Fermilab neutrino experiment E744. Opposite-sign dimuons are a clean signature of charm production and provide unique information on the strange component of the nucleon.

## I. Introduction

We present data on charm production in neutrino-nucleon scattering from Fermilab experiment E744. This experiment has high statistics and explores the energy range from 30-600 GeV. Charm is produced from  $d$  and from  $s$  quarks. However, as anti-neutrino charm production from  $\bar{d}$  quarks is suppressed by the Cabibbo angle, while production from  $\bar{s}$  quarks is not, this is a unique probe of the strange quark component of the nucleon.

## II. Charm production

Figure 1 illustrates the basic Feynmann diagrams for charm production in neutrino scattering. In the standard quark parton model the cross section for  $\nu N$  charm production is:

$$\frac{d^2\sigma^{\nu N}}{dx dy} = \frac{G_F^2 s}{2\pi} x' \left[ \sin^2 \theta_C d_N(x') + \cos^2 \theta_C s_N(x') \right] \left(1 - \frac{m_c^2}{sx'}\right) \quad (1.a)$$

$$\frac{d^2\sigma^{\bar{\nu} N}}{dx dy} = \frac{G_F^2 s}{2\pi} x' \left[ \sin^2 \theta_C \bar{d}_N(x') + \cos^2 \theta_C \bar{s}_N(x') \right] \left(1 - \frac{m_c^2}{sx'}\right) \quad (1.b)$$

In the limit of massless quarks the momentum fraction carried by the struck quark would be

$$x = \frac{Q^2}{2M\nu}$$

where  $M$  is the nucleon mass and  $\nu$  is the energy of the final state hadronic system in the lab frame. In charm production  $x$  is replaced by

$$x' = x \left(1 + \frac{m_c^2}{Q^2}\right),$$

where  $x'$  is now the momentum fraction carried by the quark with  $m_c$  the mass of the charm quark. This is the *slow rescaling* formalism.<sup>[1]</sup> The additional factor of  $(1 - m_c^2/sx')$  assures that there is sufficient center of mass energy to produce a heavy quark in the final state.

The variable  $y \equiv \nu/E_\nu$  measures the energy transferred to the hadronic system and is directly related to the center-of-mass angle,  $\theta_{CM}$ , in the quark- $\nu$  frame by  $y = \frac{1}{2}(1 - \cos \theta_{CM})$ .

The functions  $d_N(x)$ ,  $s_N(x)$ ,  $\bar{d}_N(x)$  and  $\bar{s}_N(x)$  are the probabilities that a given quark type carries  $x$  fraction of the total nucleon momentum. The *valence* distributions  $d_N(x)$  and  $u_N(x)$  are much larger than the *sea* distributions  $\bar{d}_N(x)$ ,

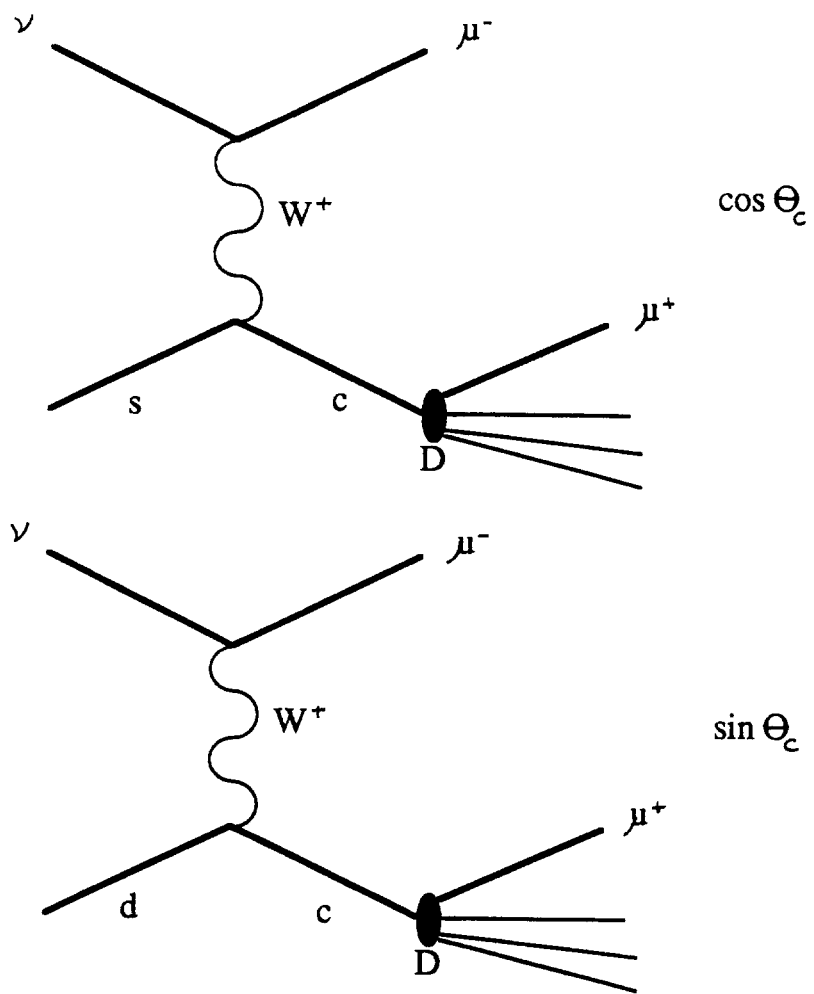


Figure 1: Diagrams for charm production.

$\bar{u}_N(x)$ , and  $s_N(x) = \bar{s}_N(x)$  which are all of similar magnitude. For simplicity the additional  $Q^2$  dependence of the quark distributions is not shown explicitly.

By convention, quark distribution functions are quoted for the proton. The notation  $q_N(x)$  used above is for an isoscalar target such as our iron calorimeter. In the following discussion the unsubscripted function  $q(x)$  will refer to the proton distribution. Isospin conservation implies that  $d_N = 1/2(d_p + d_n) = 1/2(d + u)$ . A similar relation holds for  $u_N$  and  $\bar{u}_N, \bar{d}_N$ . We assume that  $s_N = \bar{s}_N = s = \bar{s}$ . In this analysis we make no correction for Fermi motion or other nuclear effects.

Figure 2 shows the expected relative contributions of the various quark flavors to the charm production rate. These curves are derived from previous measurements of quark distributions.<sup>[2,4]</sup> Note that, due to charge conservation, charm cannot be produced from  $u$  or  $\bar{u}$  quarks. The rate for anti-neutrinos is almost directly proportional to  $\bar{s}_N(x)$  since the Cabibbo angle suppresses the  $\bar{d}_N(x)$  term. The rate for  $\nu N$  scattering is composed of approximately equal contributions from  $d_N(x)$  and  $s_N(x)$ .

We detect charm production via the semi-leptonic decay of the charm hadron which produces a second muon. The signature for charm production in our detector is thus an opposite-sign dimuon with possible additional hadronic energy.

The dimuon cross section is simply related to the total charm cross section:

$$\frac{d^2\sigma}{dx dy}(\nu N \rightarrow \mu^- \mu^+ + X) = \frac{d^2\sigma}{dx dy}(\nu N \rightarrow \mu^- + c + X) \times B_\mu \quad (2)$$

where  $B_\mu = B(c \rightarrow \mu^+ + X)$  is the average charmed hadron branching fraction into muons for the mixture of charmed hadrons produced in neutrino interactions. A study of the shapes and levels of the neutrino and anti-neutrino dimuon rates compared to the charged current rates will yield  $x d_N(x)$  and  $x s_N(x)$  and hence

(1) the ratio

$$\eta_s = \frac{2\bar{S}}{U + D} = \frac{\int 2x\bar{s}(x)dx}{\int (xu(x) + xd(x))dx}$$

or equivalently, the strange sea suppression factor

$$\kappa = \frac{2\bar{S}}{\bar{U} + \bar{D}} = \frac{\int 2x\bar{s}(x)dx}{\int (x\bar{u}(x) + x\bar{d}(x))dx}$$

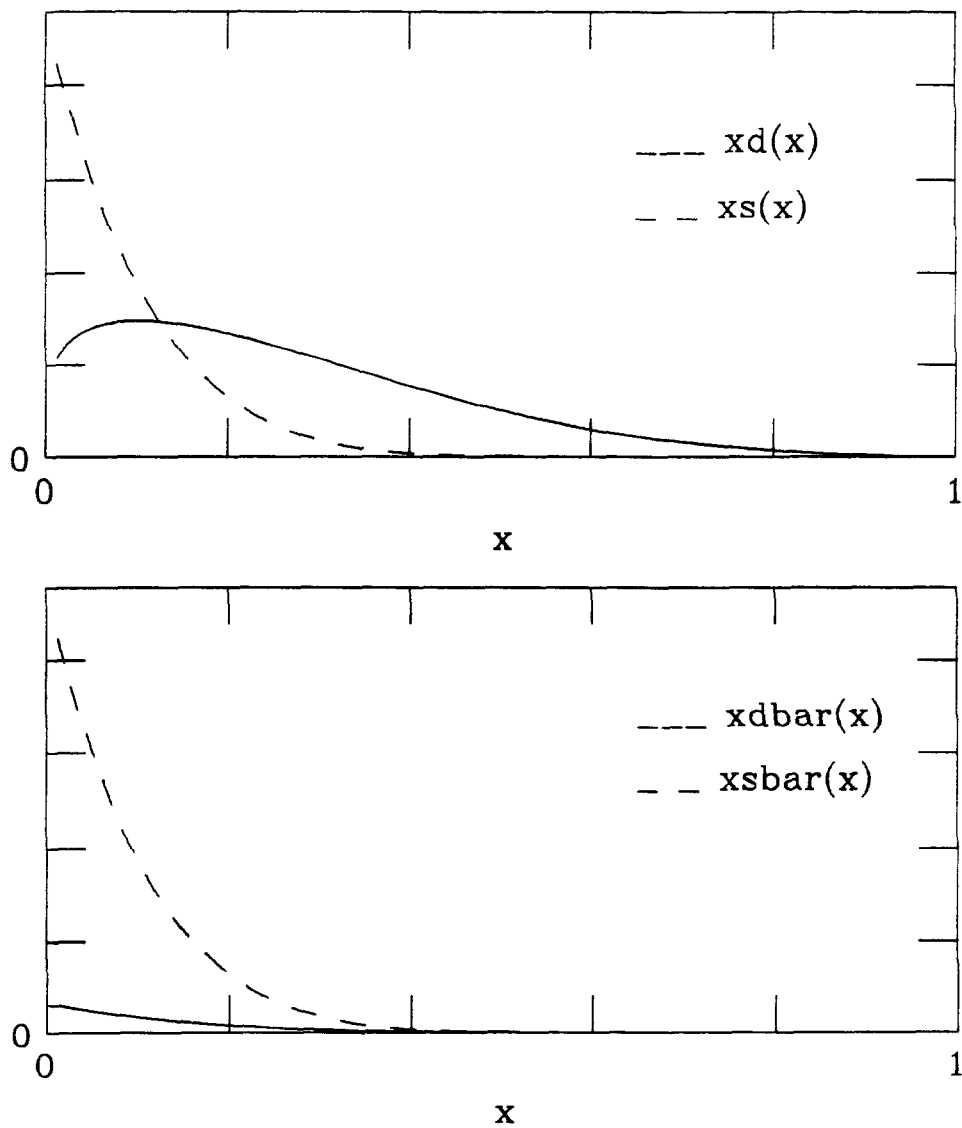


Figure 2: Contributions of partons to the charm production cross section. The solid lines are  $x d_N(x)$  and  $x \bar{d}_N(x)$  and the dashed lines are  $x s_N(x)$  and  $x \bar{s}_N(x)$ .

given the ratio  $\bar{Q}/Q = \int(x\bar{u} + x\bar{d} + x\bar{s})dx / \int(xu + xd + xs)dx = 0.175 \pm 0.012$  determined from the charged current neutrino differential cross section.<sup>[2,4]</sup> If the sea is SU(3) symmetric ( $\bar{u} = \bar{d} = \bar{s}$ ) then  $\kappa = 1$ .

- (2) a measure of the  $x$  dependence of  $s(x)$  and  $d(x)$
- (3) a measurement of the branching fraction  $B_\mu$ .

### III. Experimental details

Fermilab experiment E744 was run by the CCFR collaboration in 1985. This experiment explored dimuon production with both high statistics and at higher energies than previous experiments. A new wide band quadrupole triplet neutrino beam used the 800 GeV proton energies available at Fermilab to produce detectable neutrinos and anti-neutrinos with energies from 30–600 GeV. Figure 3 shows the measured charged current interaction spectra from the 1985 run.

The Lab E detector is composed of an unmagnetized  $3 \times 3 \times 16.5$  m<sup>3</sup> target calorimeter made up of 42 drift chambers and 84 liquid scintillation counters interleaved between 168 5 cm iron plates, followed by a muon spectrometer made up of 3 magnetized iron toroids with 5 drift chambers after each magnet and an additional 10 drift chambers downstream of the last magnet for an additional lever arm. The total mass of the target calorimeter is 690 tons. In order to ensure shower containment, we use only those events which lie within a fiducial volume which is at least 25 cm from the edges of the detector transversely, and at least 2 m of iron upstream of the spectrometer longitudinally. These cuts reduce the effective fiducial mass to approximately 400 tons. The r.m.s. hadron energy resolution in the calorimeter is  $\delta E/E = 89\%/\sqrt{E, \text{GeV}}$  while the r.m.s. muon momentum resolution is  $\delta p/p = 11\%$ . Due to the long non-magnetized calorimeter, a muon can experience an energy loss of 7–15 GeV before momentum analysis in the spectrometer. We therefore impose a lower limit of 9 GeV/c on the momenta of sign analyzed muons to assure reasonable acceptance. All CCFR dimuon rates are quoted with this cut.

In addition to conventional momentum fitting, we perform straight line fits for  $x$  and  $y$  views separately in each set of 5 drift chambers in the field free regions between the spectrometer magnets. The muon time of passage is left as a free parameter. The time for each muon track can be determined with an accuracy of 5 ns. This allows us to completely eliminate the spurious dimuons from ‘accidentals’ in which two charged current events occur in the target within the 2  $\mu$ s drift chamber gate.

In the 1985 run, 800,000 fully reconstructed charged current events passing all cuts were collected in the fiducial volume of the Lab E detector, six times the

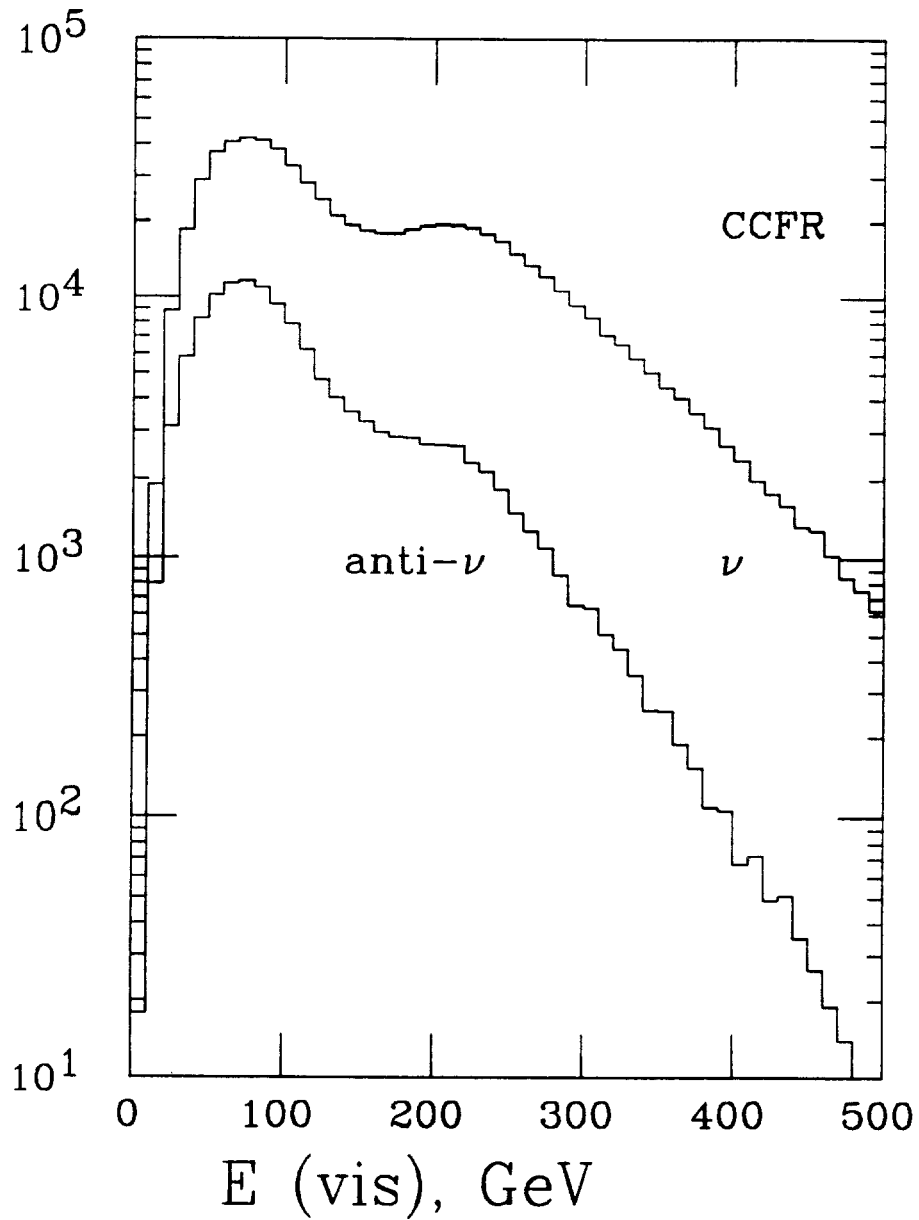


Figure 3: Measured charged current neutrino energy spectra from the 1985 Fermilab run. No acceptance correction has been made. There are 800,000 total neutrino induced events of which 65,000 have energies in the previously unstudied region above 300 GeV.

statistics of previous Fermilab experiments. All events with two calorimeter tracks entering the spectrometer were scanned for dimuons. The measured efficiency for finding dimuons with both momenta above 9 GeV/c is at least 99%. Figure 4 is a typical opposite sign dimuon event.

*Crossovers* Our beam is a 2:1 mix of  $\nu$  and  $\bar{\nu}$ . We distinguish the two by identifying the decay muon as the one with the smallest  $p_T$  relative to the hadron shower direction. The sign of the other muon then identifies the type of the incoming neutrino. Monte Carlo studies indicate that this algorithm yields a 2%  $\bar{\nu}$  contamination in the neutrino sample but a 26%  $\nu$  contamination is found in the  $\bar{\nu}$  sample. This is due to the different fluxes and kinematics for  $\nu$  and  $\bar{\nu}$  events. We also tried an alternative algorithm in which the muon of lowest momentum was assumed to be the decay muon. This algorithm yielded higher contaminations but caused no significant shift in our results. We find 1529 neutrino induced and 284 anti-neutrino induced dimuon events with the  $p_T$  classification scheme. Figure 5 shows the  $p_T$  of the decay muon and the current muon relative to the hadron shower.

#### IV. Model of opposite-sign dimuon production

##### *Charm production model*

We wish to study the relative shapes and magnitudes of  $s(x) = \bar{s}(x)$  and  $\bar{d}(x)$ . We use as our model for the total charged current rate a Buras-Gaemers<sup>[3]</sup> QCD parameterization of charged current data<sup>[4]</sup> taken with the Lab E detector in Fermilab experiments E616 and E701 at beam energies from 30-250 GeV. This parameterization yields the shapes and levels of  $u(x)$ ,  $d(x)$ ,  $\bar{u}(x)$  and  $\bar{d}(x)$ .

We describe the strange sea with two parameters,  $\eta_s$  and  $\alpha$  such that

$$\bar{s}(x) = s(x) = N_0 \bar{d}(x) (1-x)^\alpha$$

where  $N_0$  is set by the requirement that the ratio of the integrals of  $2x\bar{s}$  and  $(xu + xd)$  is  $\eta_s$ .

We must also assume a mass for the charm quark since this determines the degree of slow rescaling in the cross section. We use a central value of  $m_c = 1.5 \text{ GeV}/c^2$  and study the range from 1.0 to 1.9 GeV/c<sup>2</sup>.

##### *Decay muon kinematics*

In order to describe dimuon production in our detector, we must also model the kinematics of the decay muon. The initial charm quark fragments into a  $D$  meson or charmed baryon which carries a fraction  $z$  of the total quark

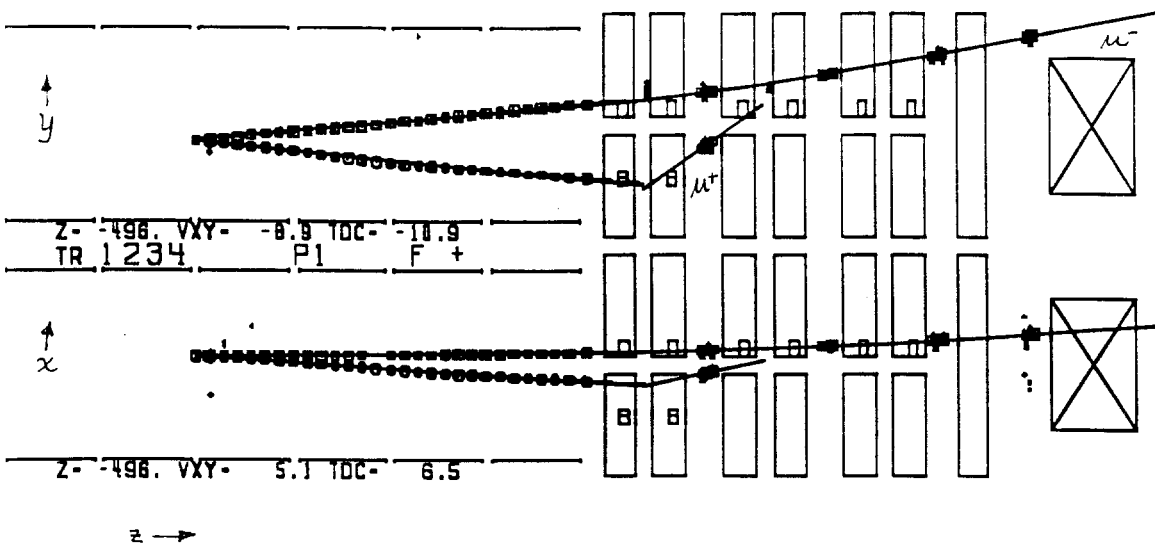


Figure 4: An opposite-sign dimuon event in the Lab E detector. The muon momenta are 57 and 14 GeV/c.

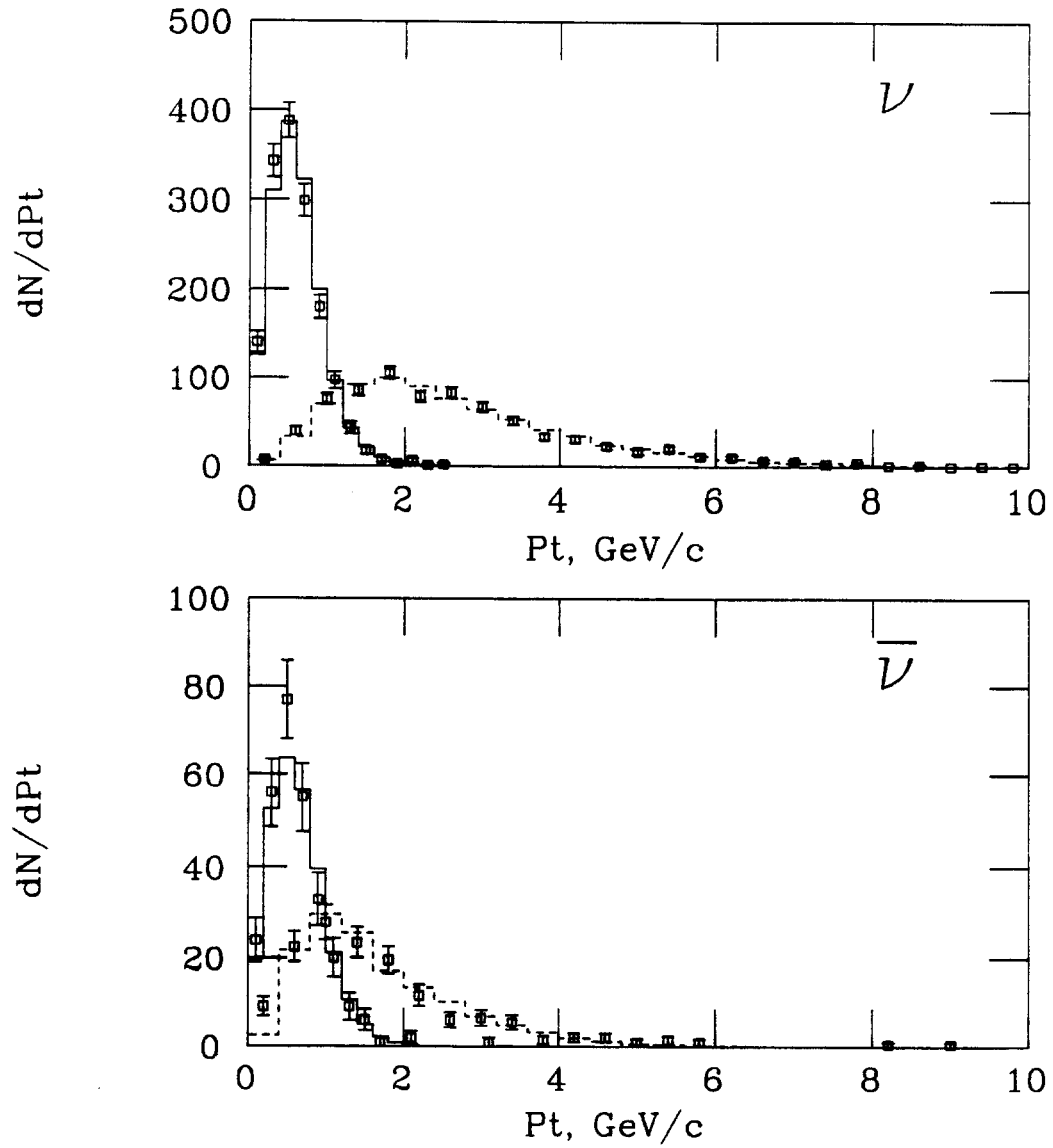


Figure 5: Solid line:  $p_T$  of the decay muon relative to the hadron shower direction. Dashed line:  $p_T$  of the current muon relative to the hadron shower direction. The squares are the data and the histogram is the Monte Carlo calculation.

momentum and acquires a  $p_T$  relative to the quark direction. The  $D$  meson then decays to produce the muon.

We use the Peterson<sup>[5]</sup> fragmentation model:

$$P(z) = \frac{1}{z(1 - \frac{1}{z} - \frac{\epsilon}{1-z})^2}$$

with  $\epsilon = .19 \pm .03$  from ARGUS<sup>[6]</sup> measurements of  $D$  fragmentation in  $e^+e^-$  scattering. In our estimate of systematic errors we vary  $\epsilon$  from 0.09 – 0.29 as the mechanism in  $\nu N$  scattering may differ from that in  $e^+e^-$ .

The  $p_T$  distribution of the charmed hadrons is:

$$\frac{dN}{dp_T^2} = e^{-1.1p_T^2}$$

from a fit<sup>[2]</sup> to LEBC hadronic charm production data.<sup>[7]</sup> The Fermilab  $\nu$ -emulsion experiment E531<sup>[8]</sup> finds that the charmed baryon component of charm production is small for  $E_\nu > 30$  GeV. We therefore treat all charm particles as  $D$  mesons in our acceptance calculation.

We use data from the Mark III collaboration<sup>[9]</sup> for the  $D$  meson decay kinematics. The branching fraction  $B_\mu = B(c \rightarrow \mu + X)$  is left as a free parameter as the precise mix of  $D^+$  and  $D^0$  mesons is unknown. A calculation based on  $e^+e^-$  data<sup>[10]</sup> and the  $D^0/D^+$  fractions measured in neutrino emulsion experiments<sup>[8]</sup> indicates that  $B_\mu$  is  $(10.9 \pm 1.4)\%$ .<sup>[2]</sup>

Figure 6 shows a comparison of the fraction of the quark energy carried by the decay muon  $z_\mu = E_{\mu_2}/(E_{\mu_2} + E_{had})$  for E744 data and for our production model.

### Background

The only significant backgrounds to the charm signal are muon production via  $\pi$  and  $K$  decay in flight within the hadron shower and trimuon production in which the third muon is not detected. We have studied these intensively as they contribute to the much rarer same-sign dimuon process.<sup>[11]</sup> We find that 6% of the opposite sign dimuons can be attributed to decay in flight and trimuons. All subsequent plots have this background subtracted.

### Cross sections

Figures 7 and 8 show the energy dependence of the total opposite sign dimuon rate after acceptance correction and background subtraction compared to the total charged current rate. The rise with energy is due to the charm mass

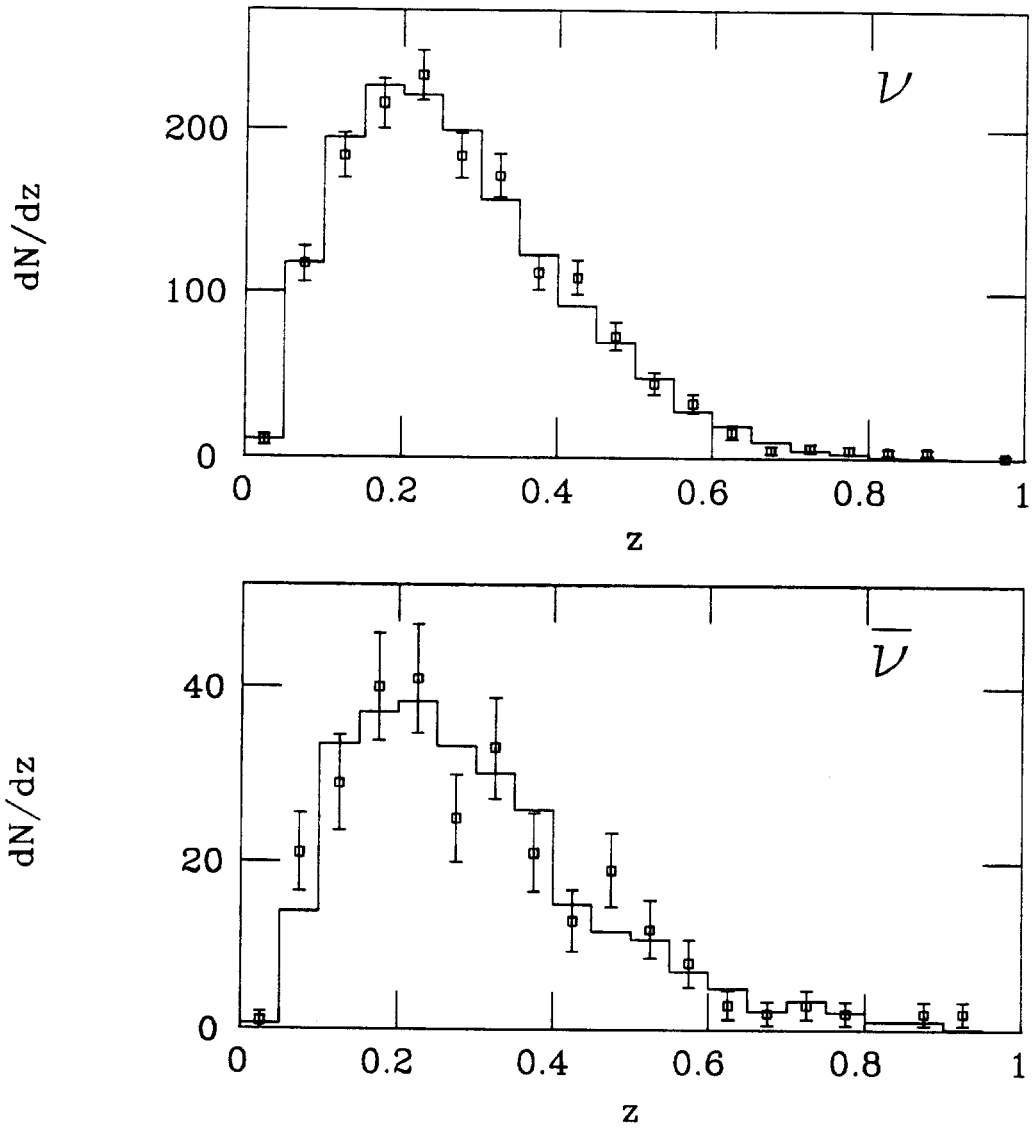


Figure 6: Comparison of  $z_\mu$  for a) neutrino and b) anti-neutrinos. The curves are the Monte Carlo simulation of dimuon production

threshold. We have used a charm mass  $m_c$  of  $1.5 \text{ GeV}/c^2$ . This experiment is compared to the CDHS measurement from CERN<sup>[12]</sup> and a previous measurement with the Lab E detector<sup>[2]</sup> in Figure 7.

#### IV. Interpretation

As shown in equations 1 and 2 the quark distribution functions can be directly related to the dimuon differential cross section  $\frac{d\sigma}{dx}$ .

We fit the  $x$  distribution from the production model to the measured distributions and extract the parameters  $\eta_s$ ,  $\alpha$  and  $B_\mu$ . Figure 9 shows such a fit while Figure 10 shows the individual components of the calculated rate, including crossovers from  $\nu \rightarrow \bar{\nu}$ .

The best fit parameters are:

$$\begin{aligned}\eta_s &= 0.068 \pm 0.011 \pm 0.005 \\ \alpha &= 4.8 \\ B_\mu &= 10.2 \pm 1.0\% \\ \chi^2 &= 9.5 \text{ for 11 degrees of freedom.}\end{aligned}$$

This implies a  $\kappa$  of  $0.46_{-0.07}^{+0.10} \pm 0.08_{-0.05} \pm 0.04$  where the first error is statistical, the second is the systematic error on  $\eta_s$  and the third error reflects the error on  $\overline{Q}/Q = 0.175 \pm 0.012$  in the conversion from  $\eta_s$  to  $\kappa$ . The details of the systematic errors are discussed below.

A similar fit (Figure 11) with  $\alpha$  constrained to zero yields  $\kappa = 0.42$  and does not describe the data as well.

**Systematic Errors** The dominant systematic errors in our measurement of  $\kappa$  are the theoretical assumptions in the acceptance modeling. If we change the charm mass from 1.0 to 1.9 GeV,  $\kappa$  varies from 0.41 to 0.54. If we vary the fragmentation parameter  $\epsilon$  from 0.09 to 0.29 ( the quoted error is  $\pm 0.03$  ),  $\kappa$  varies by  $\pm 0.01$  and  $B_\mu$  varies by  $\pm 0.8\%$ .

**Comparison with other experiments** The CDHS experiment<sup>[12]</sup> has measured  $\kappa = 0.52 \pm 0.09$ . Their errors are dominated by systematics and do not include charm mass variations.

We have measured  $\kappa$  previously<sup>[2]</sup> in earlier runs with our detector to be  $\kappa = 0.52_{-0.19}^{+0.17}$  where the dominant error is statistical. As the statistics for this earlier measurement were much less than those for the present measurement,  $B_\mu$  was fixed at  $10.9 \pm 1.4\%$  determined from Mark III branching fractions and particle fractions from  $\nu$ -emulsion data.

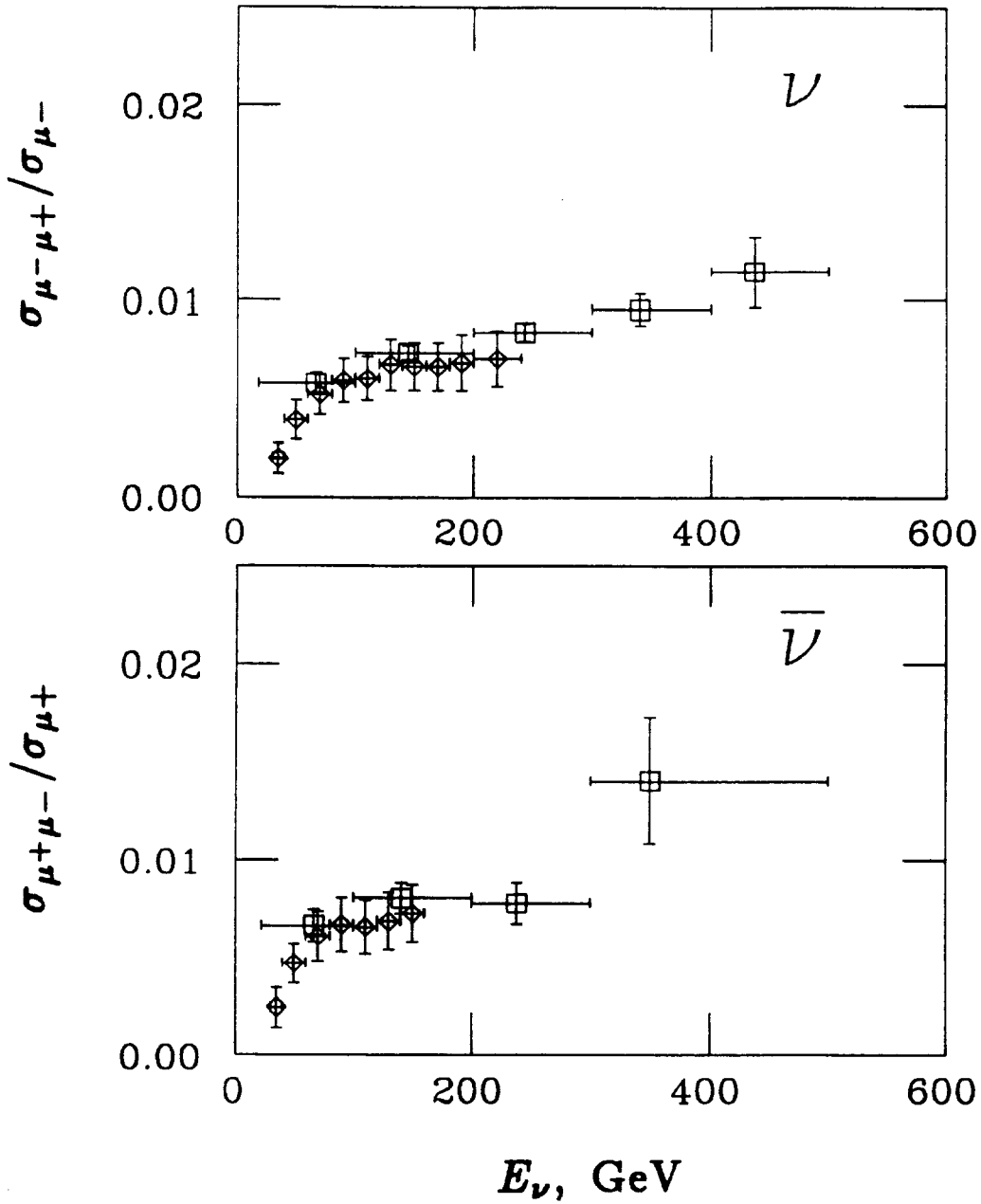


Figure 7: Dimuon rates relative to the total charged current cross section. The squares are this experiment and the diamonds are from the CDHS experiment.<sup>[12]</sup>

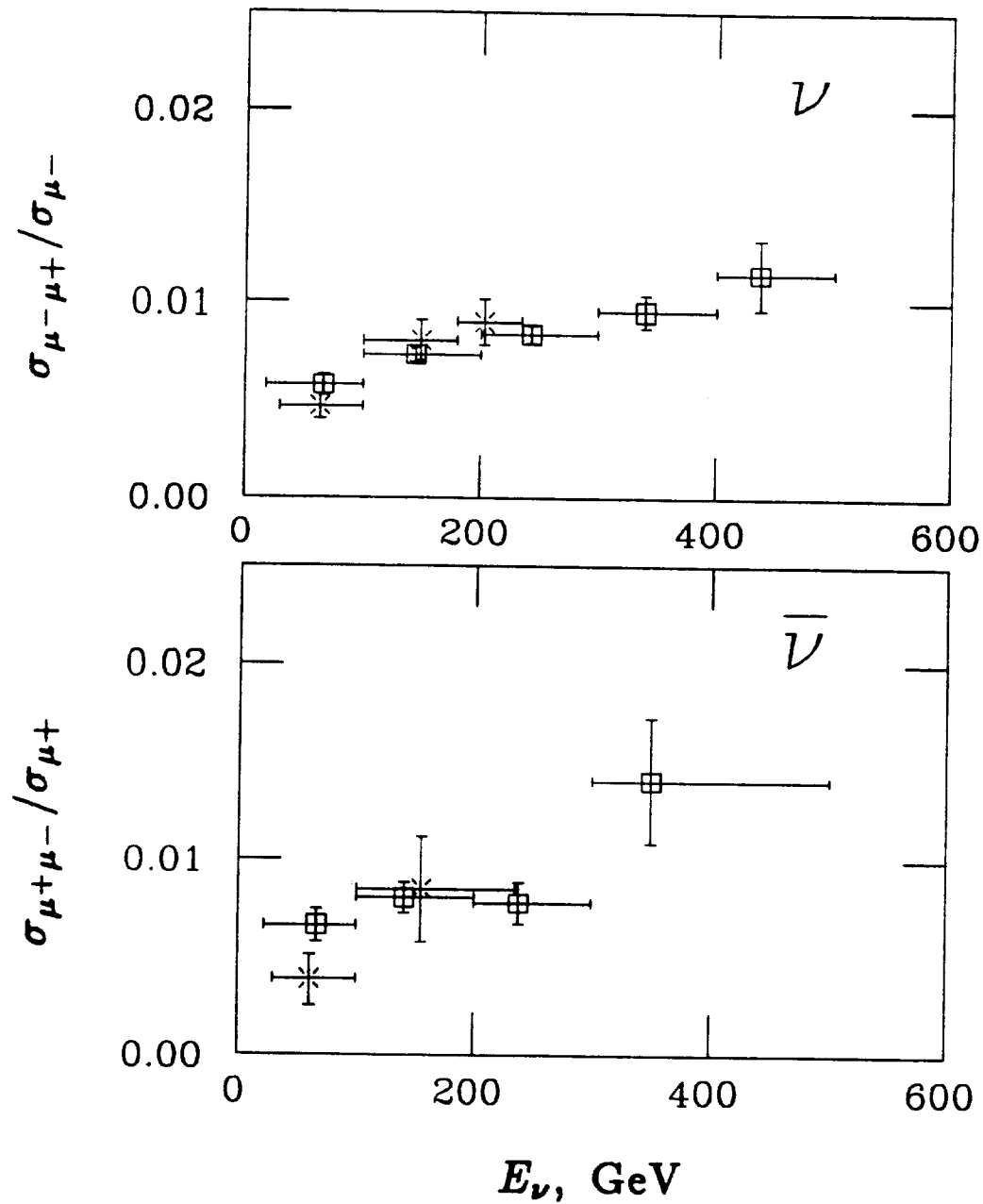


Figure 8: Dimuon rates relative to the total charged current cross section. The squares are this experiment and the crosses are from an earlier run with the same apparatus.<sup>[2]</sup>

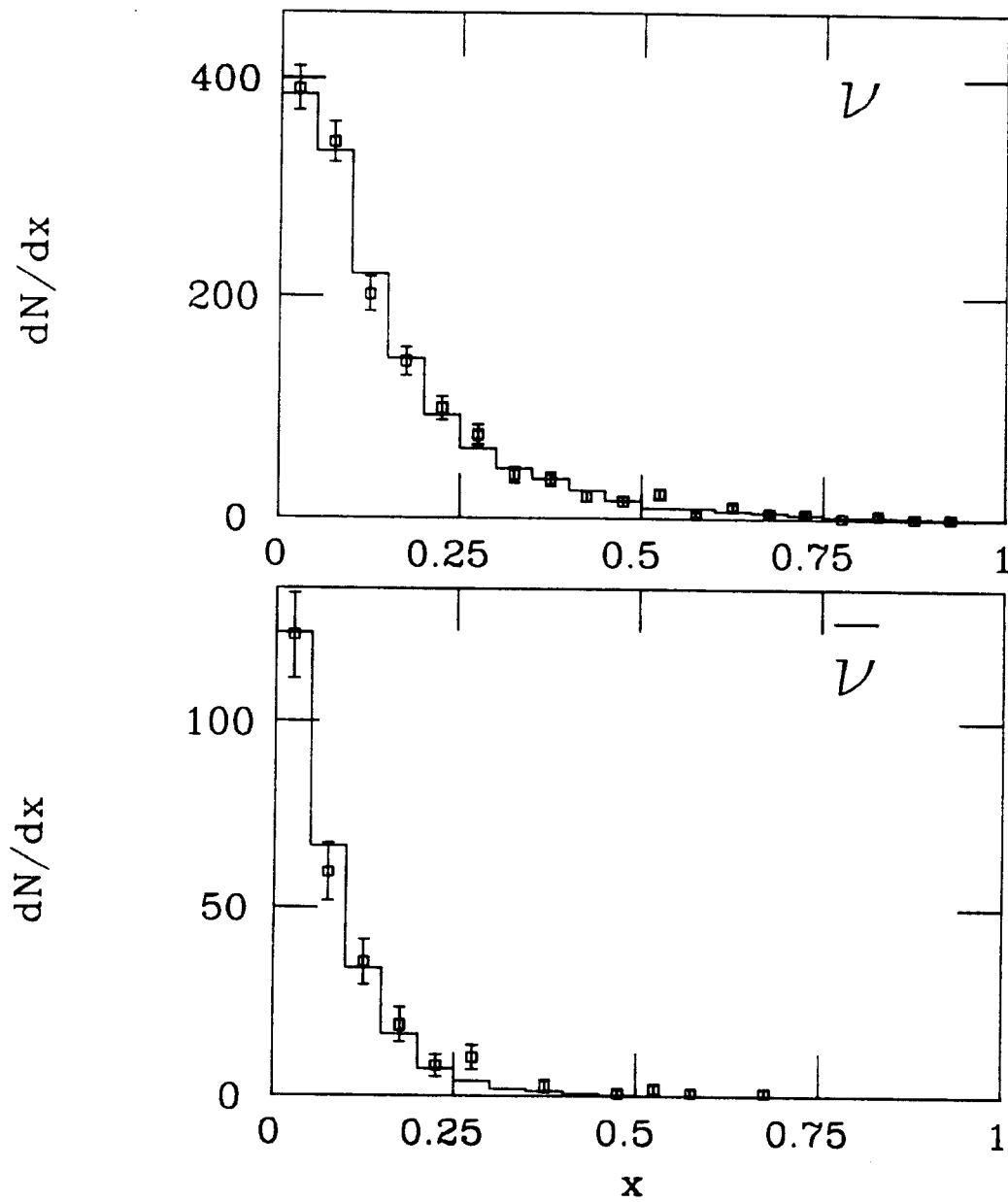


Figure 9: Simultaneous fit to  $\frac{d\sigma}{dx}$  for  $\nu$  and  $\bar{\nu}$ . The curve is the model.

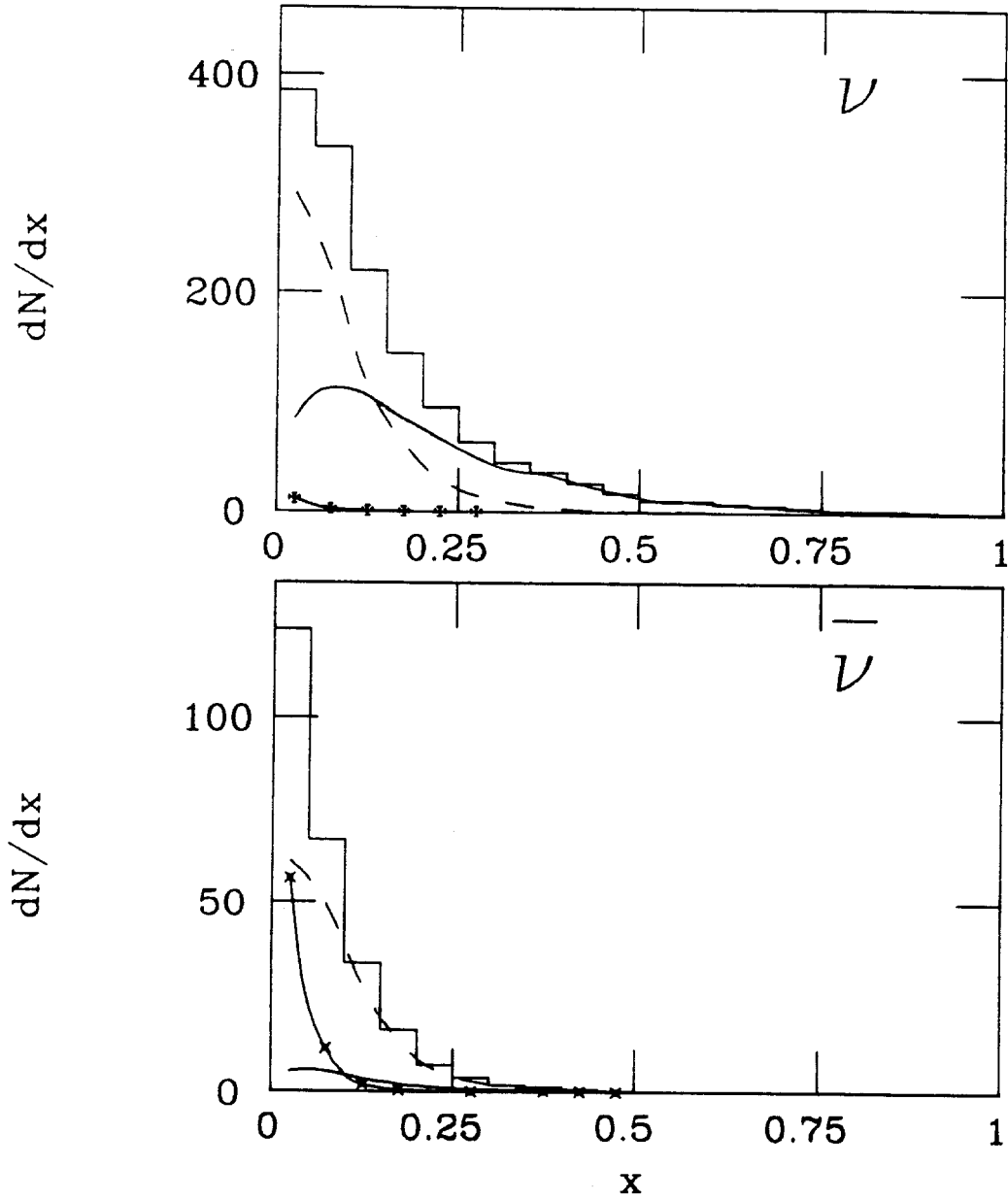


Figure 10: Components of the model. The histogram is the total calculated rate, the solid curve is the  $d_N$  quark contribution, the dashed curve is the  $s_N$  quark contribution and the curve with dots indicates the crossover component.

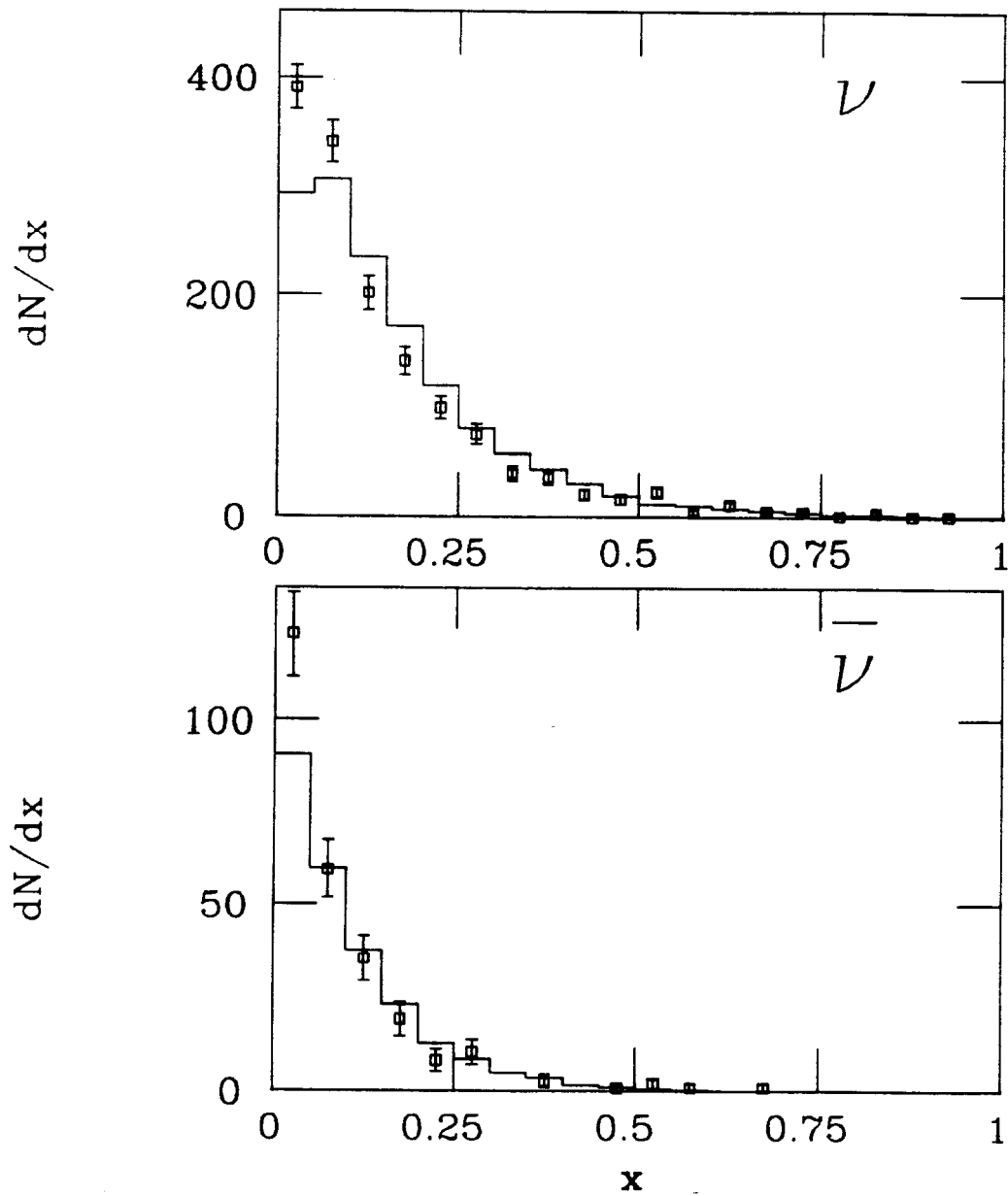


Figure 11: Simultaneous fit to  $\frac{d\sigma}{dx}$  for  $\nu$  and  $\bar{\nu}$  with  $\alpha$  constrained to zero. The curve is the model.

### Conclusion

We have studied the level and  $x$  dependence of the strange sea. We find that  $\kappa$ , which would be 1 for SU(3) symmetry is around 1/2. This value is consistent with earlier measurements.

## REFERENCES

- [1] R.N. Barnett, Phys. Rev. Lett. **36**, 1163 (1976), B.J. Edwards, T.D. Gottschalk, Nucl. Phys. **B186**, 309 (1981), C.H. Lai, Phys. Rev. **D18**, 1422 (1978), H. Georgi, H.D. Politzer, Phys. Rev. **D14**, 1829 (1976), B.J. Kaplan, F. Martin, Nucl. Phys. **B115**, 333 (1976).
- [2] K. Lang *et. al.*, Z. Phys. **C33**, 483 (1987).
- [3] A.J. Buras, K.J.F. Gaemers, Nucl. Phys. **B132**, 249 (1978).
- [4] D. MacFarlane *et. al.*, Z. Phys. **C26**, 1 (1984).
- [5] C. Peterson *et. al.*, Phys. Rev. **D27**, 105 (1983).
- [6] H. Albrecht *et. al.*, Phys. Lett. **150B**, 235 (1985).
- [7] M. Aguilar-Benitez *et. al.*, Phys. Lett. **123B**, 103 (1983).
- [8] N. Ushida *et. al.*, Phys. Lett. **121B**, 287 (1983).
- [9] D.M. Coffman, Ph.D. Thesis, California Institute of Technology, CALT-68-1415 (1987).
- [10] R.M. Baltrusaitis *et. al.*, Phys. Rev. Lett. **54**, 1976 (1985).
- [11] B.A. Schumm *et. al.*, Phys. Rev. Lett. **60**, 1618 (1988).
- [12] H. Abramowicz *et. al.*, Z. Phys. **C15**, 19 (1982).